Supporting Information

Influence of TFSI post-treatment on surface doping and passivation of lead halide perovskites

Konstantina Gkini[1], Spyros Orfanoudakis[1,2], Filippos Harlaftis[1], Panagiotis Dallas[1], Christos Kouzios[1], Polychronis Tsipas[1], Athanassios G. Kontos[2], Maria Konstantakou[1], Thomas Stergiopoulos[1,*]

[1]*Institute of Nanoscience and Nanotechnology, NCSR Demokritos, 15341, Aghia Paraskevi, Athens, Greece*

[2]*Department of Physics, School of Applied Mathematical and Physical Sciences, National Technical University of Athens, 15780, Zografou, Athens, Greece*

* Corresponding author: *t.stergiopoulos@inn.demokritos.gr*

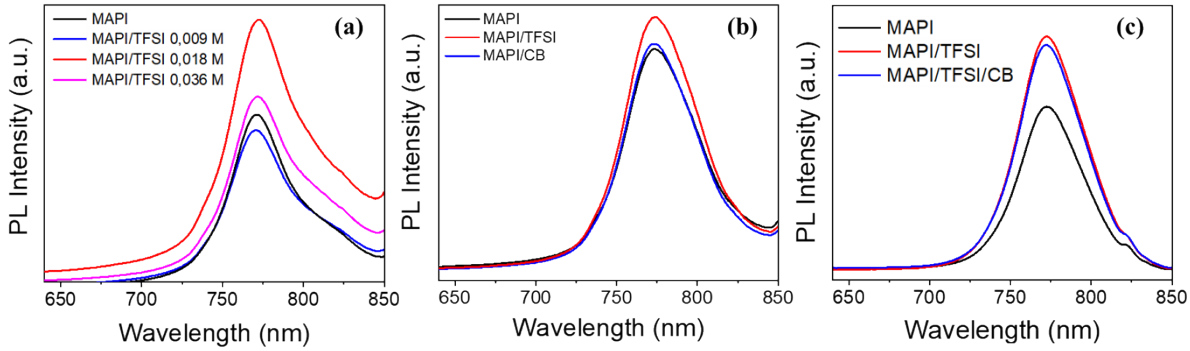

Figure S1. Steady-state PL spectra of different TFSI concentrations in chlorobenzene spin-coated on glass/MAPI substrates (a), FTO/MAPI films before and after TFSI and chlorobenzene (CB) deposition (b), and FTO/MAPI/TFSI films before and after washing with CB by spin-coating (c).

XPS spectra justified the successful TFSI deposition on top of the perovskite film, depicting peaks arising from F1s, S2p and N1s binding energies (Fig. S2). Specifically, the F1s spectrum (Fig. S2a) demonstrates a peak at 689.5 eV which is attributed to the -CF3 group of TFSI anion. The corresponding peak at 169.5 eV of the S2p spectrum (Fig. S2b) is difficult to be discerned, maybe due to the material's very low concentration. Regarding the imide anion of the TFSI molecule, the peak at 400.7 eV of N1s spectrum (Fig.S2c) is related to it. For comparison purposes, both MAPI and MAPI/TFSI N1s spectra are presented.

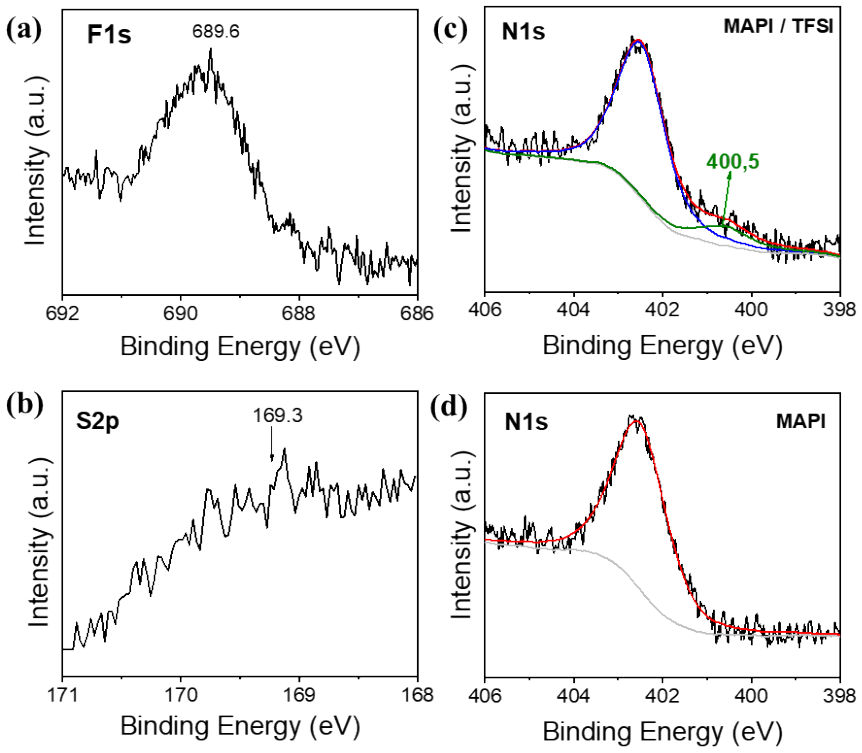

Figure S2. F1s (a), S2p (b), N1s (c) XPS spectra of MAPI/TFSI films and N1s spectrum (d) of MAPI film.

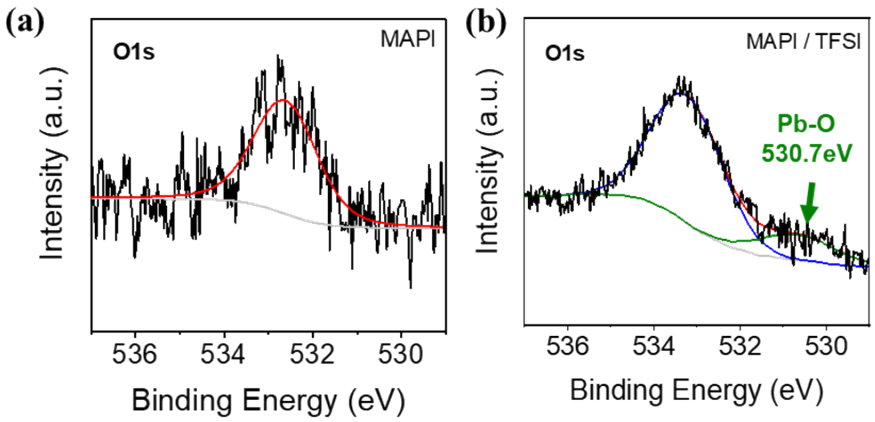

Figure S3. O1s XPS spectra of MAPI (a) and MAPI/TFSI (b), respectively.

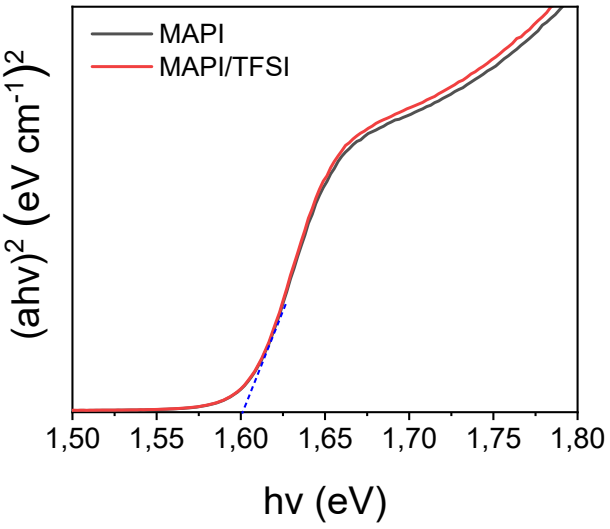

Figure S4. Tauc plots of FTO/TiO_2/MAPI films before and after TFSI deposition, from which the optical bandgap of the perovskite films is extracted.

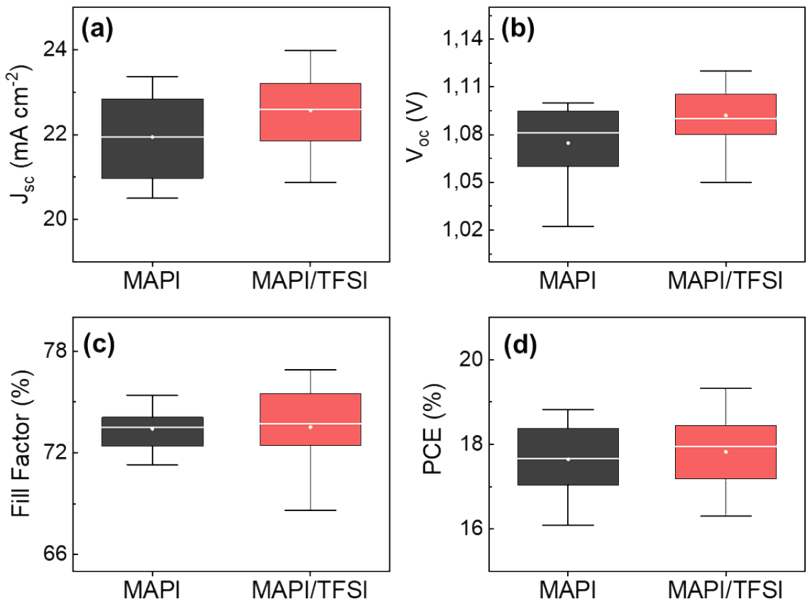

Figure S5. Statistical analysis of the photovoltaic parameters for the reference and TFSI-based planar PSCs.

TFSI was dissolved in chlorobenzene in three different concentrations (0.05mgml^{-1}, 0.1mgml^{-1} and 0.5mgml^{-1}) and used as antisolvent during MAPI film fabrication. The results, as presented in the following graph, show that the lowest concentration leads to improved performance, compared to the reference device, but not better than that of the

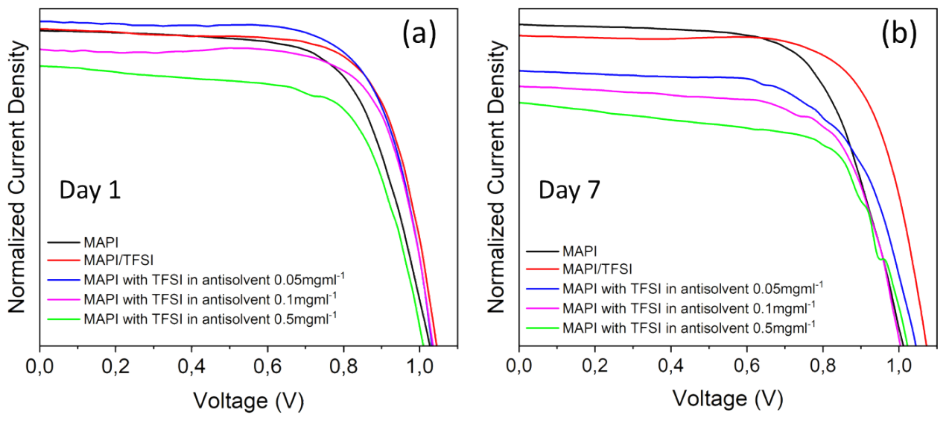

TFSI based device. But after 7 days, when the samples were measured again, all concentrations are far worse than the reference device.

Figure S6. Stabilized PCE at maximum power point for planar PSCs with and without TFSI passivation

We also fabricated TFSI treated MAPI devices and performed a comparison experiment between Spiro-OMeTAD HTL without LiTFSI additive (or any other TFSI based additive) and Spiro-OMeTAD with LiTFSI and TBP as additives. Both kind of samples were left overnight in desiccator so as the Spiro to be oxidized. The results were quite interesting as the first day of measurements the non-TFSI HTL based devices showed a very deteriorated performance, but after some days it was significantly improved. However, after the 9^{th} day when its short-circuit current density exceeded that of the Li-TFSI based device, its FF was still very low.

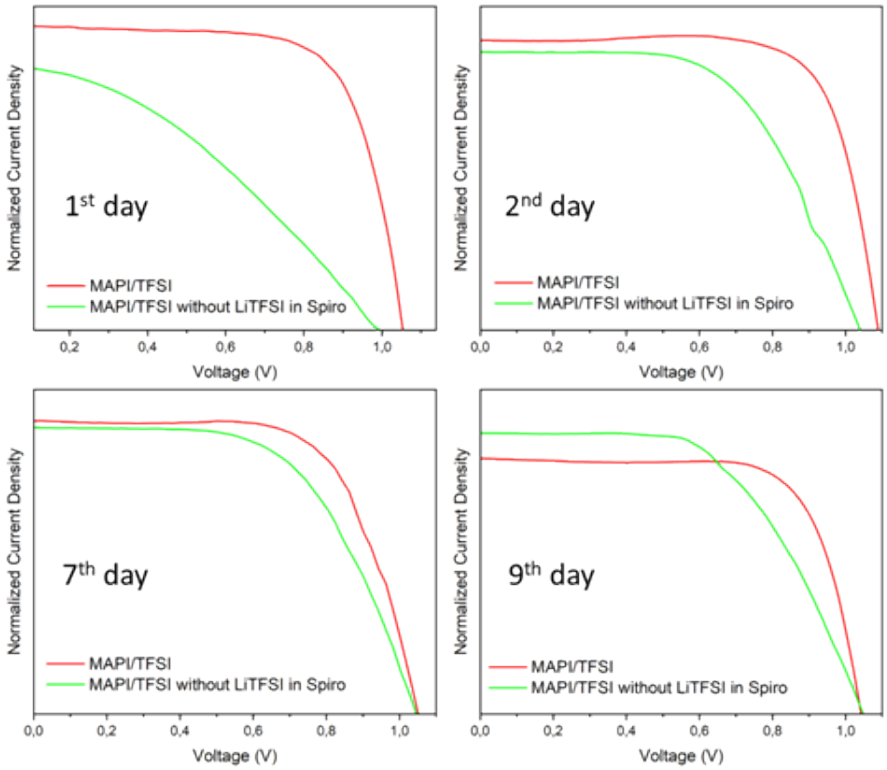

Figure S7. Stabilized PCE at maximum power point for planar PSCs with and without TFSI passivation

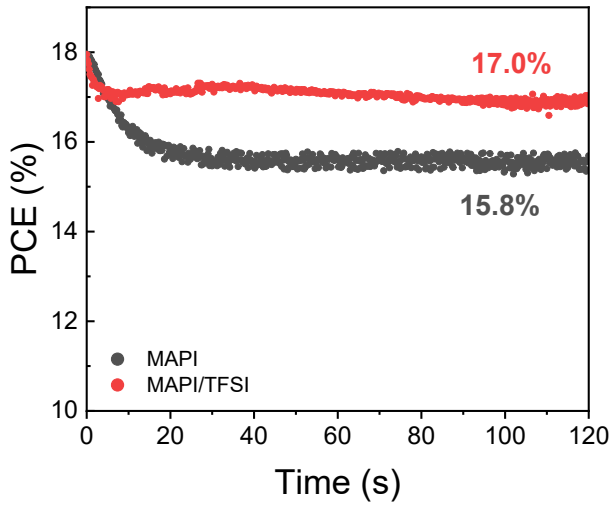

Figure S8. Stabilized PCE at maximum power point for planar PSCs with and without TFSI passivation.

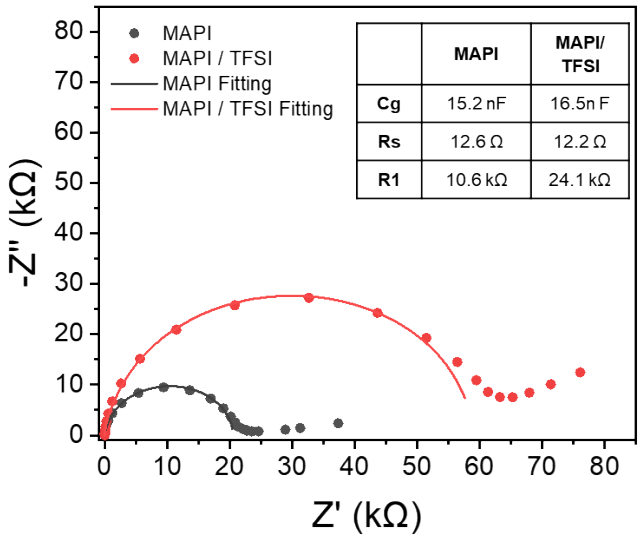

	MAPI	MAPI/ TFSI
Cg	15.2 nF	16.5n F
Rs	12.6 Ω	12.2 Ω
R1	10.6 kΩ	24.1 kΩ

Figure S9. Impedance spectra (Nyquist plots) obtained for planar PSCs (with and without TFSI passivation) αt 0V in the dark. The inset table includes the values of the geometric capacitance, the series resistance and the recombination resistance which were extracted after fitting of the spectra with an equivalent electrical circuit (the solid lines represent the fitting).

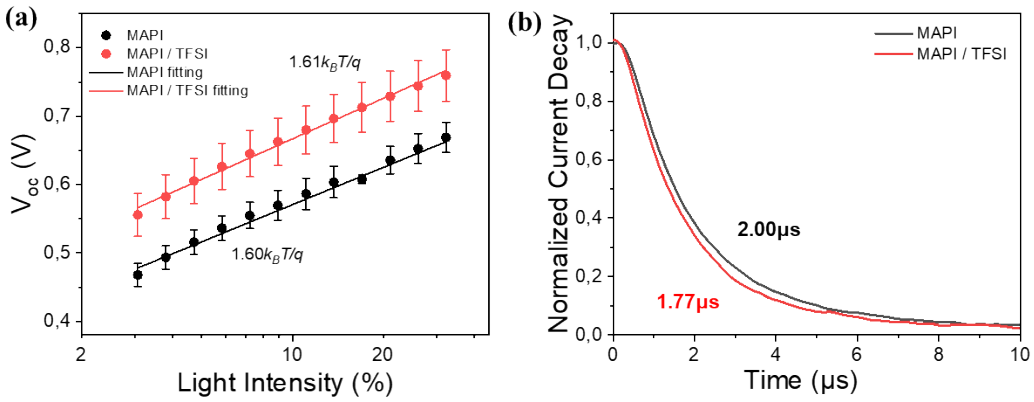

Figure S10. Light-intensity dependence of V_{OC} (extracted fromTPV experiments) (a) TPC decays (b) for planar PSCs with and without TFSI passivation.

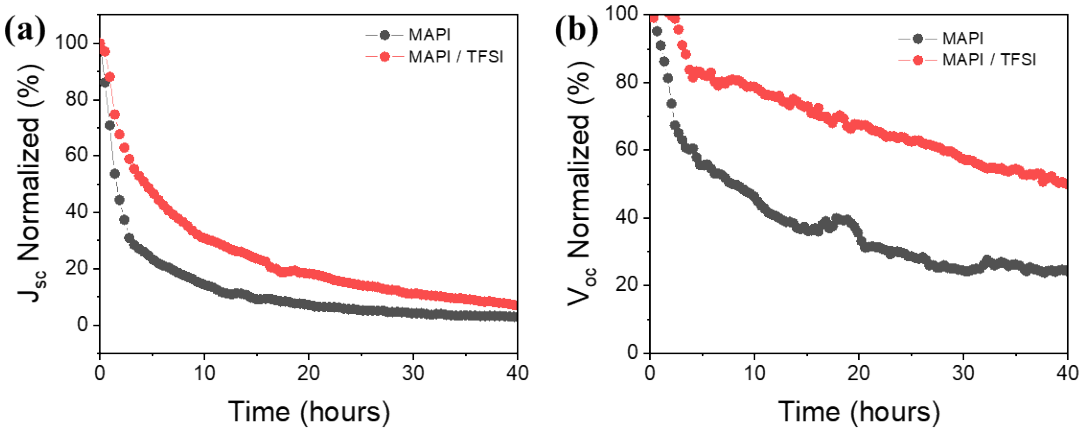

Figure S11. (a) J_{sc} and (b) V_{oc} evolution for devices (with and without TFSI) after light (1 sun illumination) stress.

Table S1. The TRPL parameters using a bi-exponential fitting for the FTO/MAPI films, with and without TFSI passivation.

sample	τ_1	A_1	τ_2	A_2	τ_{av}
MAPI	5.1 ns	0.55	37.9 ns	0.45	19.5 ns
MAPI/TFSI	6.2 ns	0.41	60.7 ns	0.59	38.1 ns

Table S2. Comparison of the photovoltaic parameters for reference and TFSI based planar devices under forward (FS) and reverse (RS) scan. Calculated hysteresis index for both devices is also presented.

sample	J_{sc} (mA cm^{-2})	V_{oc} (V)	FF (%)	PCE (%)	HI
MAPI_RS	21.30	1.09	76.4	17.8	0.18
MAPI_FS	21.00	1.06	64.3	14.3	
MAPI/TFSI_RS	23.55	1.13	73.3	19.4	0.12
MAPI/TFSI_FS	23.27	1.09	64.5	16.4	

Table S3. Photovoltaic parameters of 30 reference planar MAPI devices.

sample	J_{sc} (mA cm^{-2})	V_{oc} (V)	FF (%)	PCE (%)
MAPI	22.35	1.09	71.3	17.4
	23.32	1.10	73.5	18.8
	22.87	1.10	74.1	18.6
	22.80	1.07	72.7	17.7
	22.84	1.08	75.1	18.5
	21.10	1.04	73.3	16.1
	20.87	1.03	75.6	16.3
	22.16	1.10	73.8	18.0
	20.90	1.09	74.6	17.0
	21.73	1.09	72.0	17.1
	23.28	1.06	70.4	17.4
	22.84	1.03	69.5	16.3
	22.43	1.02	69.7	15.9
	22.57	1.10	71.8	17.8
	21.20	1.04	70.3	15.5
	21.39	1.07	68.9	15.8
	23.18	1.11	71.6	18.4
	21.65	1.06	69.8	16.1
	22.41	1.12	68.9	17.3
	20.58	1.09	74.0	16.7
	21.53	1.10	72.1	17.3
	21.23	1.04	73.2	16.8
	22.11	1.11	71.7	17.6
	21.47	1.11	73.3	14.4
	21.68	1.04	71.4	16.2
	22.41	1.07	71.7	17.3
	20.16	1.06	71.4	15.3
	20.86	1.11	72.8	16.9
	20.78	1.08	73.2	16.4
	21.30	1.09	76.4	17.8

Table S4. Photovoltaic parameters of 30 TFSI-modified MAPI devices.

sample	J_{sc} (mA cm^{-2})	V_{oc} (V)	FF (%)	PCE (%)
MAPI/TFSI	22.37	1.11	72.5	18.0
	23.77	1.12	69.0	18.4
	23.16	1.12	68.6	17.8
	22.13	1.10	74.0	18.1
	21.94	1.08	72.3	17.2
	22.79	1.10	71.4	17.9
	23.90	1.08	73.0	18.9
	23.24	1.08	71.4	18.5
	22.38	1.12	73.7	18.5
	22.97	1.09	73.7	18.5
	23.00	1.11	75.4	19.3
	21.19	1.07	74.7	16.9
	22.97	1.09	73.7	18.5
	23.05	1.09	68.7	17.3
	22.97	1.12	69.9	17.9
	22.45	1.09	70.9	17.3
	22.94	1.10	70.4	17.8
	23.55	1.13	73.3	19.4
	23.09	1.05	70.2	17.0
	21.75	1.04	71.8	16.3
	21.40	1.09	73.0	17.0
	21.81	1.10	71.4	17.2
	23.22	1.12	70.9	18.4
	21.85	1,09	72.5	17.3
	21.80	1.12	72.3	17.7
	22.07	1.09	72.3	17.5
	21.77	1.04	72.5	16.4
	21.50	1.10	76.9	18.2
	23.77	1.10	70.9	18.5
	23.51	1.10	72.5	18.8